

Graphene Based Transmitarray for Terahertz Applications

Hend A. Malhat^{1, *}, Saber H. Zainud-Deen², and Shaymaa M. Gaber³

Abstract—Circularly polarized graphene based transmitarray for terahertz applications is proposed. The characteristics of the graphene material is explained. The cell element of the transmitarray is made of square Quartz cell. Dual circular graphene rings are printed on both sides of the Quartz substrate. The graphene ring radius is varied to change the transmission coefficient phase and magnitude. The effect of the graphene chemical potential on the transmission coefficient is demonstrated. Transmitarray is composed of 9×9 unit cell elements. A circularly polarized circular horn is used to feed the transmitarray at $f = 6$ THz. The left- and right-hand field components in the E - and H -plane are determined. The variation of the gain and the axial-ratio with the frequency are explained. The peak gain is 18.63 dB and 1-dB gain bandwidth is 6.8%. The transmitarray produces a circular polarization from 5.5 THz to 6.5 THz.

1. INTRODUCTION

Rapidly developing terahertz (THz) science and technology has attracted a great deal of attention in recent years due to its enormous potential such as in spectroscopy, communication, defense, and biomedical imaging. Graphene, a flat monolayer of carbon atoms tightly packed in a two-dimensional honeycomb lattice, has recently attracted the attention of the research community due to its novel mechanical, thermal, chemical, electronic and optical properties [1]. Graphene is a promising material for the realization of miniaturized resonant THz antennas [2]. It supports surface plasmon polaritons in the THz range, which are widely tunable by a change of graphene's electrochemical potential via chemical doping, or magnetic field or electrostatic gating. Because of its unique characteristics, graphene is envisaged to enable new potential applications, ranging from ultra-high-speed transistors to transparent solar cells [3]. High gain antennas are desired in various applications, such as satellite communications, radar systems, and radio astronomy observations [4]. Traditionally, large parabolic reflectors and lenses antennas are selected for the systems mentioned above. However, these antennas are bulky, heavy, and their geometrical shape tends to be distorted during the implementation. The use of graphene for dynamically control the phase of reflectarray and transmitarray antennas at THz frequencies has been proposed for the first time at [5]. Tunable graphene reflective cells for THz reflectarray is proposed in [6]. In this paper, transmitarray antennas are introduced for these applications. In transmitarray, there is no ground plane as in the reflectarray case so, the incident electromagnetic waves pass through the transmitarray structure and converted from spherical wave into a plane wave [7–9]. Consequently, the feed horn cannot interfere with the transmitted and received waves, and there is no blockage loss. The transmitarray has many surface antenna elements, each of which imparts the necessary phase shift to equalize the path length of every ray. In this antenna, however, there is no ground plane. Therefore, the feed signal is not reflected, but passes through the structure as it is collimated into a plane wave. The disadvantage with this antenna, however, is that its design is more complicated than that of a reflectarray since both the phase and transmission properties of the element must be considered [10].

Received 7 May 2014, Accepted 18 June 2014, Scheduled 21 June 2014

* Corresponding author: Hend Abd Malhat (er_honida1@yahoo.com).

¹ Faculty of Electronic Engineering, Menoufia University, Egypt. ² Faculty of Electronic Engineering, Menoufia University, Egypt.

³ Egyptian Russian University, Egypt.

The unit-cell design in the transmitarray assumes normal incident wave on each element. However, in the real case the incident wave on the elements at the array edges has an angle different from the normal (which is an approximation). Many transmitarray researches had been proposed using different antenna elements for different applications [11–13]. In this paper, circularly polarized graphene based transmitarray at $f = 6$ THz is designed. The transmitarray is composed of 9×9 unit-cell elements and is covering an area of $225 \times 225 \mu\text{m}^2$. The radiation characteristics of the transmitarray are demonstrated. Full-wave analysis using the FIT technique for the antenna structure is illustrated [14].

2. GRAPHENE THEORY

The optical properties of the graphene monolayer can be represented by sheet with surface conductivity, $\sigma(\omega)$, which is derived from the Kubo formula [15].

$$\sigma(\omega) = \sigma_{intra}(\omega) + \sigma_{inter}(\omega) \quad (1)$$

It consists of an intraband contribution:

$$\sigma_{intra}(\omega, \mu_c, \Gamma, T) \approx -j \frac{q_e^2 K_B T}{\pi \hbar (\omega - j2\Gamma)} \times \left(\frac{\mu_c}{K_B T} + 2 \ln \left(e^{-\mu_c/K_B T} + 1 \right) \right) \quad (2)$$

and an interband contribution:

$$\sigma_{inter}(\omega, \mu_c, \Gamma, T) \approx j \frac{q_e^2}{4\pi \hbar} \left(\frac{2|\mu_c| - (\omega + j\tau^{-1})\hbar}{2|\mu_c| + (\omega + j\tau^{-1})\hbar} \right) \quad (3)$$

where j is the imaginary unit, q_e the electron charge, \hbar the reduced Plank constant, K_B the Boltzmann's constant, τ the transport relaxation time, T the temperature, μ_c the chemical potential, ω the operating angular frequency, and scattering rate $\Gamma = 1/2\tau$ represents loss mechanism. The intraband term of the conductivity given by (2) is a reasonable approximation in the frequency range below 8 THz [15]. The graphene chemical potential, μ_c , depends on carrier density, which can be controlled by gate voltage, electric bias field, and/or chemical doping. By increasing μ_c the graphene surface conductivity is increased, and the resonances are shifted for higher frequencies. Within the random-phase approximation, the surface conductivity of graphene can be represented in a local, Drude-like form. The Drude model assumes that charge carriers in a material scatter frequently as they move through the medium [16]. This diffusive model of transport reduces the characterization of the transport to two parameters: the number of charge carriers (n) and the ease with which they move through the material (quantified as either mobility, mean scattering time, or mean free path). However, the Drude model is generally valid for graphene samples because the mean free paths are still significantly shorter than typical sample sizes. The effective surface conductivity of graphene is generally a complex quantity and can be expressed as $\sigma = \sigma_r + j\sigma_i$ where σ_r and σ_i are the real and imaginary parts of the effective conductivity, respectively. Therefore, from Maxwell's equations one can show that the real and imaginary parts of the relative complex permittivity $\varepsilon = \varepsilon' + j\varepsilon''$ can be expressed as [16]

$$\varepsilon' = 1 + \frac{\sigma_i}{\omega \varepsilon_o \Delta}, \quad \text{and} \quad \varepsilon'' = \frac{\sigma_r}{\omega \varepsilon_o \Delta} \quad (4)$$

where ε_o is the permittivity of the vacuum and Δ the graphene layer thickness. For the purpose of 3-D simulation, the thickness of graphene is assumed to be $\Delta = 1$ nm, although other extremely small values for this thickness lead to similar results. If the imaginary part of the effective conductivity is assumed to be zero then the real part of the complex permittivity ε' is equal to the relative permittivity as in metals such as a copper and gold (low frequency regime).

3. DESIGN OF UNIT-CELL

The configuration of the proposed transmitarray unit cell is shown in Fig. 1. The cell element of the transmitarray consists of square Quartz cell, with length $L_c = 25 \mu\text{m}$, substrate thickness $h_c = 20 \mu\text{m}$ with $\varepsilon_r = 3.45$, and $\tan \delta = 0.004$. Dual circular graphene rings are printed on both sides of the Quartz substrate. Each circular graphene ring has width $t = 1 \mu\text{m}$ and thickness $\Delta = 1$ nm. The outer graphene ring has radius R_o and the inner graphene circular ring have radius of R_i with ($R_i = 0.5R_o$).

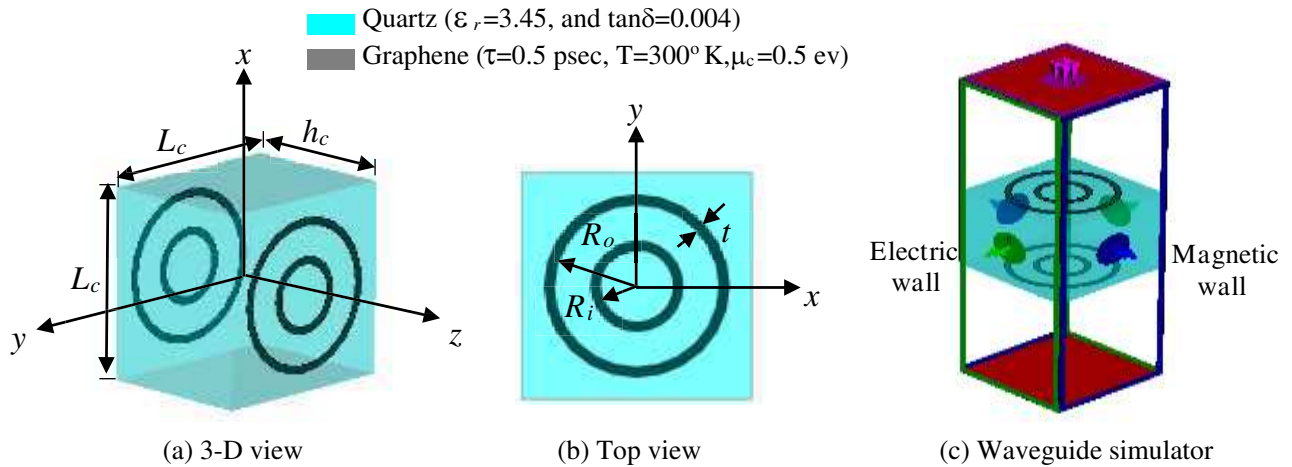


Figure 1. Detailed construction of the proposed unit-cell.

The graphene material parameters are $\tau = 1$ psec, $T = 300^\circ\text{K}$, and $\mu_c = 0.5$ ev which result in surface impedance of $17 + j214.2\Omega$.

To calculate the relation between the transmission coefficient phase and the graphene ring radius variation in the unit cell, the unit cell is placed in a waveguide simulator [7]. The unit cell is positioned in the middle of the waveguide simulator as shown in Fig. 1(c). The perfect electric and magnetic wall boundary conditions are applied to the sides of the surrounding waveguide, and result in image planes on all sides of the unit cell to represent an infinite array approximation. A plane wave was used as the excitation of the unit cells inside the waveguide simulator and only normal incidence angle was considered. There are several limitations to the infinite array approach. *First*, all elements of the transmitarray are identical; this is clearly not the case in the real transmitarray in which the radii of the graphene rings in each cell element must vary according to the required phase compensation. *Secondly*, the transmitarray itself is not infinite in extent. The relationship between variable circular graphene ring radius and the transmission coefficient at 6 THz was determined using the FIT technique as shown in Fig. 2. The unit cell that having only ring radius variation from $3\ \mu\text{m}$ to $8.5\ \mu\text{m}$ produce a phase shift ranging from 0° to 355° , with the transmission coefficient magnitude changes from -4.8 dB to 0 dB. The surface conductivity of the graphene material with different chemical potentials μ_c at $\tau = 1$ psec and $T = 300^\circ\text{K}$ is shown in Fig. 3.

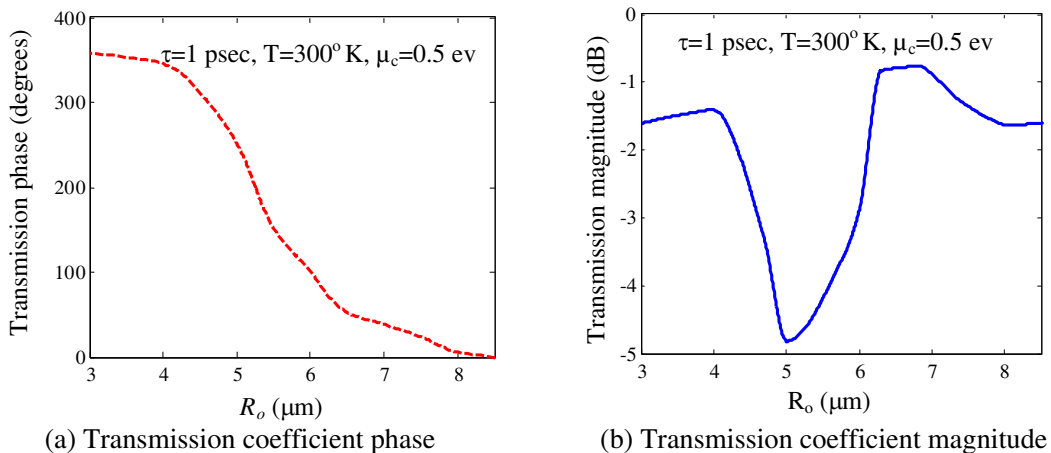


Figure 2. Variation of the transmission coefficient phase and magnitude versus the graphene ring radius at $f = 6$ THz.

In the frequency range of interest, from 2 to 7 THz, the intraband contribution of the conductivity dominates, and the interband contribution can be ignored. By altering the chemical potential from 0 eV to 0.95 eV, the complex conductivity has been calculated using Eq. (2). The conductivity is decreased with increasing frequency. At a constant frequency, the graphene conductivity is increased with increasing the chemical potential μ_c . The graphene layer surface impedance $Z_s = 1/\sigma$, behaves as a constant resistance in series with an inductive reactance that increases with frequency. At 6 THz the surface impedance (resistance and inductive reactance) is decreased with increasing the chemical potential μ_c . A parametric study on the influence of graphene material parameters μ_c at $\tau = 1$ psec and $T = 300^\circ\text{K}$ on the variation of the transmission coefficient phase and magnitude versus the graphene ring radius is presented in Fig. 4. As the graphene chemical potential μ_c is increased the transmission coefficient phase variation is increased to approach 360° and the transmission magnitude is reduced at some values. There will be a compromise between the transmission coefficient phase and magnitude variation for each value of graphene chemical potential μ_c . For $\mu_c = 0$ eV and $\mu_c = 0.19$ eV the conductivity of the graphene layer is almost constant with frequency. So, by changing the graphene ring radius at constant frequency 6 THz the variation in the phase of the transmitted wave is nearly constant and part of the incident plane wave is reflected back from the graphene layer. By increasing

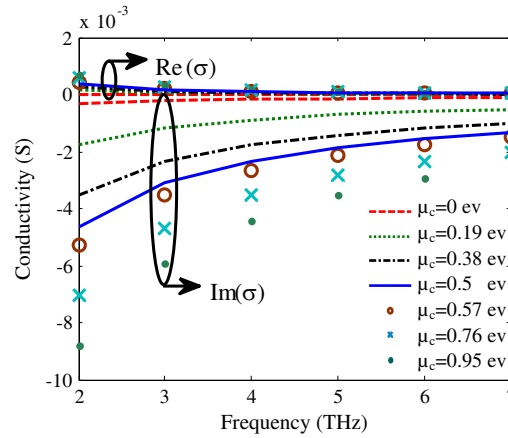


Figure 3. Graphene complex conductivity versus frequency with different chemical potentials μ_c at $\tau = 1$ psec and $T = 300^\circ\text{K}$.

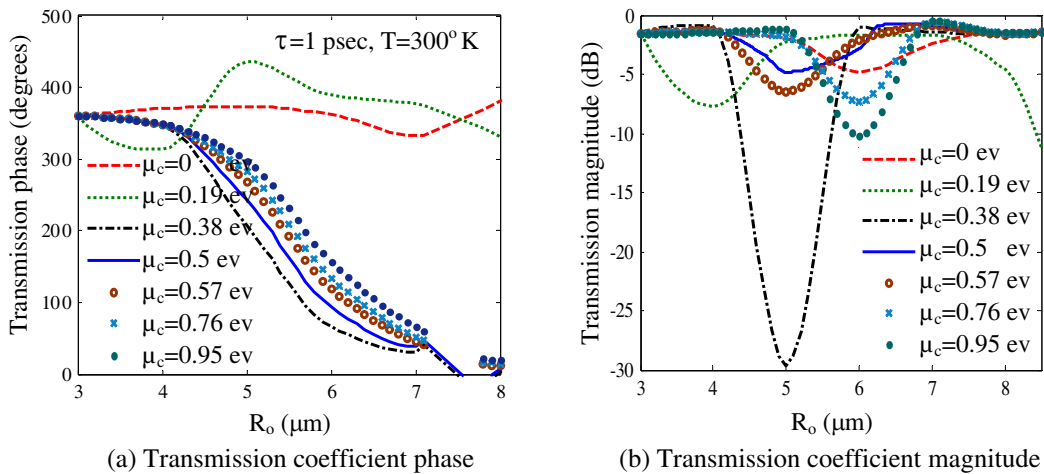


Figure 4. The variation of the transmission coefficient phase and magnitude versus the graphene ring radius for different graphene nobilities at $f = 6$ THz.

the chemical potential, the variance of the graphene conductivity is remarkable from the beginning to the remnant of the frequency band which results in a noteworthy variety of the transmitted wave phase. The slope of the transmission coefficient phase variation curve is reduced by increasing the chemical potential which improves the final transmitarray bandwidth. While the fluctuation of the transmission coefficient magnitude didn't follow a specific blueprint.

4. TRANSMITARRAY ANTENNA

Generally, the transmitarray transforms the spherical wave emanating from the feed into a plane wave at the output, as conventional parabolic reflector antenna. Consider an array on the x - y plane illuminated by a feed horn as shown in Fig. 5(a). The required phase compensation distribution φ_o at each unit cell element in the transmitarray to collimate a beam in the (θ_o, ϕ_o) direction is obtained by [7]:

$$\varphi_o(x_{cij}, y_{cij}) = k_o [d_{ij} - x_{cij} \sin(\theta_o) \cos(\phi_o) - y_{cij} \sin(\theta_o) \sin(\phi_o)] \quad (5)$$

$$d_{ij} = \sqrt{(x_{cij} - x_f)^2 + (y_{cij} - y_f)^2 + z_f^2} \quad (6)$$

where $k_o = 2\pi/\lambda_o$ is the propagation constant in free space; $(x_{cij}, y_{cij}, 0)$ are the coordinates of transmitarray unit cell element; (x_f, y_f, z_f) are the coordinates of the phase centre of the feed horn. This equation depends on estimating the extra distance travelled by the incident plane wave and transmitted back from a planar reflector than that transmitted back from a parabolic reflector to transform the spherical wave to a plane wave collimating the beam in the required direction.

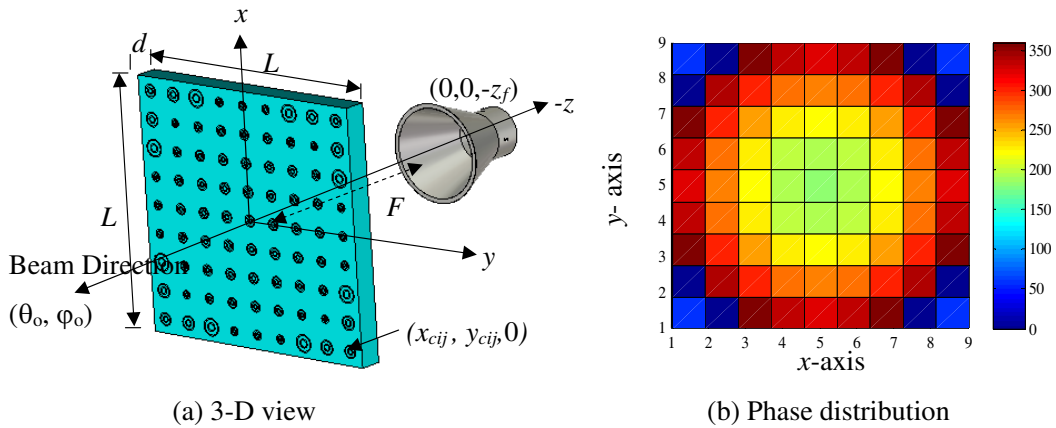


Figure 5. Configuration of 9×9 graphene based transmitarray fed by circularly polarized circular horn and the required phase compensation for each element.

The phase of the transmitted wave of each element is achieved by varying the element dimensions. The phase shift of each cell element in the transmitarray should be between 0 and 360° with magnitude variation from 0 to -4 dB. The transmitarray used in this analysis is composed of 9×9 unit cell elements and is covering an area of $225 \times 225 \mu\text{m}^2$ in x - y plane. Of course, larger number of cells can be used to get higher gain. However, it is the computing facilities which limited the number of cells to 9×9 . A common voltage is applied to all the graphene rings to obtain a typical chemical potential ($\mu_c = 0.5$ eV) to be the same for all the rings. The compensation phase distribution for the 9×9 transmitarray elements is shown in Fig. 5(b). The transmitarray is symmetrical around both the x -axis and y -axis with phase distribution varies from 0 to 360° . A circular horn is used to feed the transmitarray with radius $R_h = 40 \mu\text{m}$, and length $L_h = 56 \mu\text{m}$ at 6 THz as shown in Fig. 6(a). The horn is fed via two orthogonal coaxial probes with 90° phase shift to produce circular polarization (CP) field from the horn. The horn is located at a distance of $225 \mu\text{m}$ from the transmitarray aperture. The 3-D radiation pattern of the circular horn is shown in Fig. 6(b) at 6 THz. The left-hand (LHCP) and right-hand (RHCP) circular polarization far-fields for the circular horn and the transmitarray in E -plane and H -plane are shown in Fig. 7 at $f = 6$ THz. The program used in computations is based on full-wave analysis of the problem and is taking into consideration the effect of the mutual coupling between the elements

and the edge effects of the array. The cross-polar (right-hand circular polarization) level is lower than -50 dB relative to the copolar in the H -plane axial direction at the designed frequency. The side lobe levels (SLL) in the E - and H -planes are approximately -15 dB. The gain of the transmitarray against the frequency is shown in Fig. 8(a). The peak gain is 18.63 dB. The 1 dB gain bandwidth is 0.41 THz

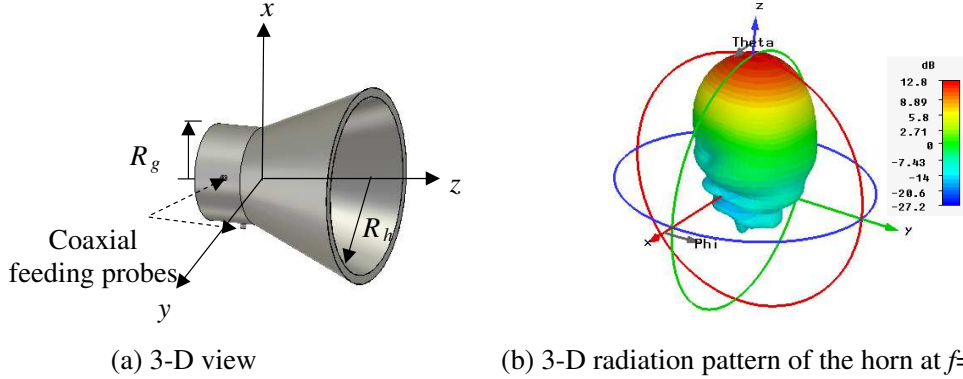


Figure 6. Detailed construction of a circularly polarized circular horn antenna and its 3-D gain pattern at $f = 6$ THz.

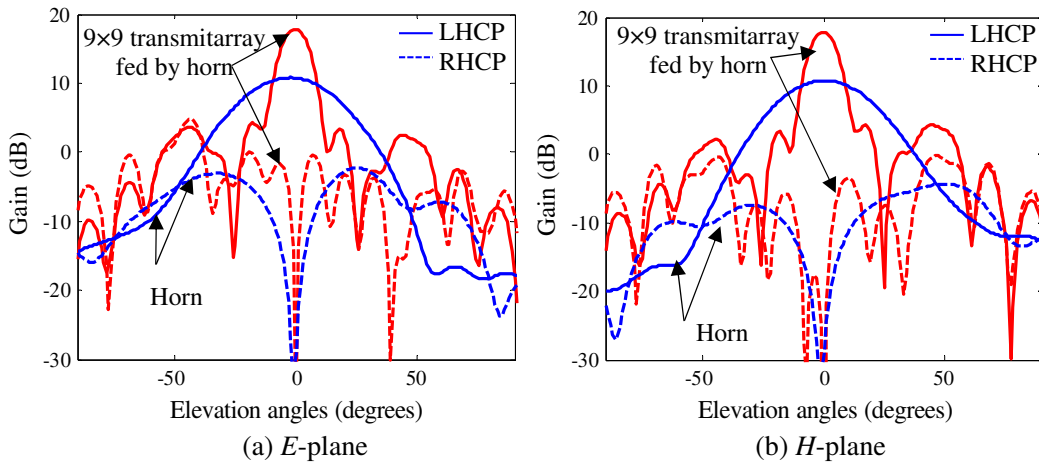


Figure 7. The configuration of 9×9 graphene based transmitarray fed by circularly polarized horn at $f = 6$ THz.

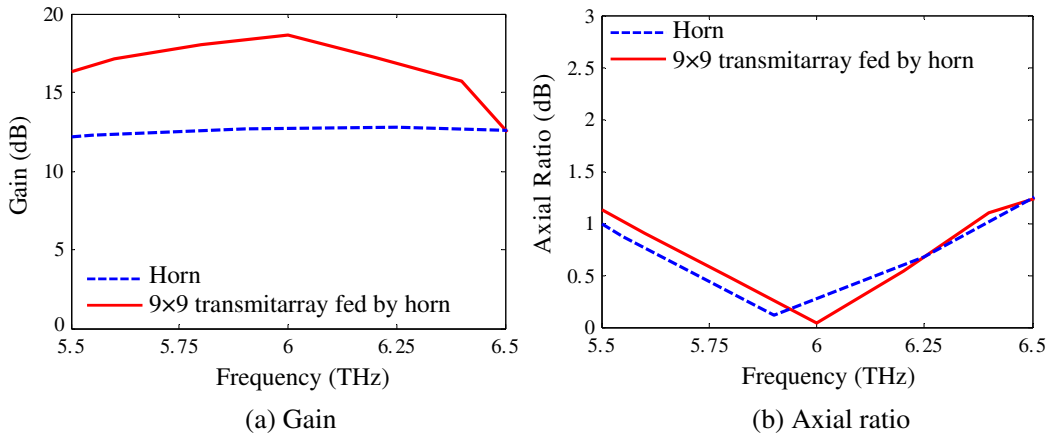


Figure 8. The gain and axial ratio variation versus frequency for 9×9 graphene based transmitarray fed by circularly polarized horn at $\theta = \varphi = 0$.

(6.8%). The axial ratio versus frequency is shown in Fig. 8(b). The array produces circular polarization in the axial direction with axial ratio, $AR < 1$ dB and covers a range from 5.5 THz to 6.5 THz.

5. CONCLUSION

In this paper, terahertz transmitarray with graphene ring elements has been proposed. Circularly polarized horn antenna is used to feed the transmitarray. The effect of changing the radius of the ring element and the graphene chemical potential on the transmission coefficient of the cell element has been explained. The circularly polarized field components are calculated using the full-wave analysis of the antenna structure. The gain of the antenna at the boresight direction has been found 18.63 dB with gain bandwidth equal to 6.8%.

REFERENCES

1. Choi, W. and J. Lee, *Graphene: Synthesis and Applications*, CRC Press Taylor & Francis Group, NW, USA, 2012.
2. Bao, W., "Electrical and mechanical properties of graphene," Ph.D Thesis, University of California Riverside, USA, 2012.
3. Jian, L., "Graphene and its hybrid nanostructures for nanoelectronics and energy applications," Ph.D Thesis, University of California Riverside, USA, 2011.
4. Hansen, R. C., *Phased Array Antennas*, John Wiley & Sons, Inc., Hoboken, NJ, USA, 2009.
5. Hum, S. V. and J. Perruisseau-Carrier, "Reconfigurable reflectarray and array lenses for dynamic antenna beam control: A review," *IEEE Transactions on Antennas and Propagation*, Vol. 62, No. 1, 183–198, Jan. 2014.
6. Rodrigo, D., L. Jofre, and J. Perruisseau-Carrier, "Unit cell for frequency-tunable beamscanning reflectarrays," *IEEE Transactions on Antennas and Propagation*, Vol. 61, No. 12, 5992–5999, 2013.
7. Gaber, S. M., "Analysis and design of reflectarrays/transmitarrays antennas," Ph.D Thesis, Minoufiya University, 2013.
8. Huang, J. and J. A. Encinar, *Reflectarray Antennas*, Wiley-IEEE Press, Pisataway, NJ, 2007.
9. Zainud-Deen, S. H., H. A. Malhat, S. M. Gaber, and K. H. Awadalla, "Perforated nanoantenna reflectarray," *Progress In Electromagnetics Research M*, Vol. 29, 253–265, 2013.
10. Zainud-Deen, S. H., H. A. Malhat, S. M. Gaber, and K. H. Awadalla, "Plasma reflectarray," *Plasmonic Journal*, Vol. 8, 1469–1475, 2013.
11. Zainud-Deen, S. H., H. A. Malhat, S. M. Gaber, and K. H. Awadalla, "Beam steering plasma reflectarray/transmitarray antennas," *Plasmonic Journal*, DOI 10.1007/s11468-013-9645-4, 2013.
12. Lau, J. Y. and S. V. Hum, "Reconfigurable transmitarray design approaches for beamforming applications," *IEEE Transactions on Antennas and Propagation*, Vol. 60, No. 12, 5679–5689, Dec. 2012.
13. Lau, J. Y. and S. V. Hum, "A wideband reconfigurable transmitarray element," *IEEE Transactions on Antennas and Propagation*, Vol. 60, No. 3, 1303–1311, Mar. 2012.
14. Cooke, S. J., R. Shtokhamer, A. A. Mondelli, and B. Levush, "A finite integration method for conformal, structure-grid, electromagnetic simulation," *Journal of Computational Physics*, Vol. 215, 321–347, 2006.
15. Rouhi, N., S. Capdevila, D. Jain, K. Zand, Y. Wang, E. Brown, L. Jofre, and P. Burke, "Terahertz graphene optics," *Nano Research Journal*, Vol. 5, No. 10, 667–678, Oct. 2012.
16. Kadhom, M. J., J. S. Aziz, and R. S. Fyath, "Performance investigation of loop and helical carbon nanotube antennas," *Journal of Emerging Trends in Computing and Information Sciences*, Vol. 3, No. 12, 1606–1613, Dec. 2012.